How to cite: *Angew. Chem. Int. Ed.* **2023**, *62*, e202308678
doi.org/10.1002/anie.202308678

Main Group Chemistry

Diboriranide σ-Complexes of d- and p-Block Metals

*Philipp Grewelinger, Tim Wiesmeier, Carsten Präsang, Bernd Morgenstern, and David Scheschkewitz**

Abstract: Diboriranides are the smallest conceivable monoanionic aromatic cycles, yet only limited examples have been reported and their reactivity and complexation behavior remain completely unexplored. We report a straightforward synthesis of the first peraryl diboriranide c-$(DurB)_2CPh^-$ as its lithium salt in three steps via the corresponding non-classical diborirane from a readily available 1,2-dichlorodiborane(4) (Dur = 2,3,5,6-tetramethylphenyl). With the preparation and complete characterization of representative complexes with tin, copper, gold and zinc, we demonstrate the strong preference of the diboriranide for σ-type coordination modes towards main group and transition metal centers under unperturbed retention of the three-membered B_2C-ring's $2e^-$ π-system.

Introduction

The coordination chemistry of aromatic species such as benzene,[1] cyclopentadienide anions[2] and tropylium cations[3] is dominated by the dative bonding of the π-system to electron-deficient acceptors from the p- and the d-block of the periodic table. The isoelectronic replacement of carbon atoms of the ring systems by one or two boron atoms led to various examples of borole dianions,[4] boratabenzenes[5] and diboratabenzenes[6] as well as the seven-membered borepins.[7] While monoanionic boratabenzenes and neutral borepins are employed as conceptually obvious substitutes for cyclopentadienide ligands, the dianionic species allow for a straightforward access to various triple decker complexes.[8] In comparison, the coordination chemistry of three-membered aromatics is much less developed: Although the all-carbon cyclopropenium cations **I** (Scheme 1) have been employed as ligands, they predominantly react under reductive ring-opening, in other words oxidative addition of the σ-framework to the transition metal.[9] Borirenes **II**, formally derived by isoelectronic replacement of one carbon by a boron atom, have enjoyed particular attention due to the convenient access by borylene transfer to alkynes.[10] This methodology also provides facile access to borirenes in X-type coordination to transition metals,[11] but the coordination to transition metals as L-type ligands is rare and occurs exclusively in the η^3-mode through the π-system.[12]

While a few diboriranides **III** were described by Berndt et al.,[13] triborirandiides **IV** have only been known as homoaromatic derivatives[14] until Braunschweig et al. reported a monocyclic example in 2015.[15] Stable complexes with d- and p-block elements are unknown in both cases. In fact, even the general reactivity of diboriranides **III** is an almost unchartered terrain, presumably due to (a) the relatively bulky substitution patterns in all known examples and (b) the rather complicated access, typically in multi-step procedures and/or poor yields.

The first diboriranides reported by Berndt et al. in 1985 had been prepared by excessive reduction of 1,1-bis(chloroboryl)-2,2-bis(trimethylsilyl)alkene.[13a] In this reaction, the boryl-substituted end of the C=C bond becomes part of the anionic B_2C ring and the silyl-substituted end is transformed into an exocyclic methyl group with an additional anionic charge that can be selectively protonated to give **A** (Scheme 2). While the procedure requires only three

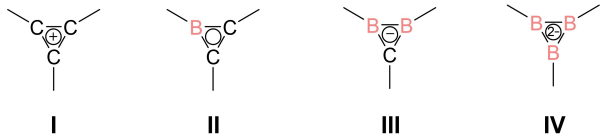

Scheme 1. Schematic representation of isoelectronic cyclopropenium analogues with boron atoms.

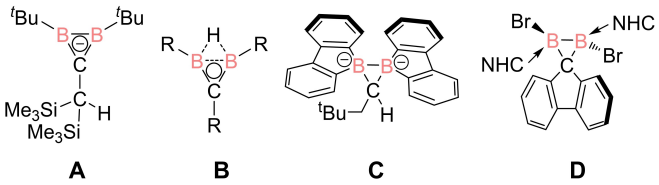

Scheme 2. Previously reported B_2C ring structures (NHC = 1,3-diisopropyl-4,5-dimethylimidazol-2-ylidene).

[*] M. Sc. P. Grewelinger, B. Sc. T. Wiesmeier, Dr. C. Präsang, Prof. Dr. D. Scheschkewitz
Krupp-Chair for General and Inorganic Chemistry, Saarland University
66123 Saarbrücken (Germany)
E-mail: scheschkewitz@mx.uni-saarland.de
Dr. B. Morgenstern
Service Center X-ray diffraction, Saarland University
66123 Saarbrücken (Germany)

steps from a 1,2-dichlorodiborane(4), it is inherently limited in scope. All other diboriranides reported after 1985 have been prepared from neutral diboriranes **B** by reductive cleavage of the B–B-bridging hydrogen atom, allegedly as hydride.[16]

The procedures, however, often involve more than six steps from 1,2-dichlorodiboranes(4), result in mediocre yields and lack general applicability.[13a,17] For example, aromatic substituents at the ring carbon atom remain inaccessible, thus precluding any extension of the conjugated system for the exploitation of the peculiar electronic properties in extended systems. The same limitation applies to the two classical diboriranes **C** and **D** reported by the groups of Wagner[18] and Liu,[19] which are inherently unsuitable as precursors for diboriranides anyway due to the tetracoordinate ring carbon atoms and the absence of a suitable leaving group in this position.

We now report the straightforward and high yielding synthesis of a simple diboriranide with a sterically innocent and potentially conjugated phenyl substituent at the ring carbon atom in three steps from a readily available 1,2-diaryl-1,2-dichlorodiborane(4). As we will show, the coordination of the thus obtained diboriranide to p- and d-block elements is dominated by the B–B σ-bond leaving the $2e^-$ π-system essentially unperturbed and resulting without exception in species with an anti-van't Hoff/Le Bel-geometry at the boron centers.

Results and Discussion

Synthesis of lithium diboriranide

Carbon atoms in α-position to an electron deficient boron center can readily be deprotonated to result in the corresponding methyleneborates with a B–C double bond.[20] We therefore anticipated that the restrictions mentioned above may be overcome by the deprotonation of a suitably substituted derivative of a 1-methyl-2-halodiborane(4) and subsequent ring closure to the corresponding diborirane under salt elimination. Instead of the parent methyl, we opted for a benzyl group to further facilitate deprotonation and provide minimal kinetic stabilization while still maintaining a relative steric innocence and - at the same time - extending the conjugated system of the diboriranide by a phenyl substituent.

The required 1-benzyl-2-chloro-1,2-diduryldiborane(4) **1** was prepared by the surprisingly selective reaction of 1,2-dichloro-1,2-diduryldiborane(4)[21] with one equivalent of benzyl magnesium chloride[22] at −78 °C in 97 % yield. It was characterized by multinuclear NMR spectroscopy and single crystal x-ray diffraction (see Supporting Info). The deprotonation of **1** in benzylic position is indeed possible using lithium tetramethylpiperidide (LiTMP) and results in instant ring closure to the non-classical diborirane **2** (Scheme 3), which was isolated from a concentrated toluene solution at −23 °C as colorless crystals in 85 % yield. The ^{11}B NMR chemical shift at δ = 25.7 ppm is very similar to those of the previously reported diboriranes with duryl substituents at the

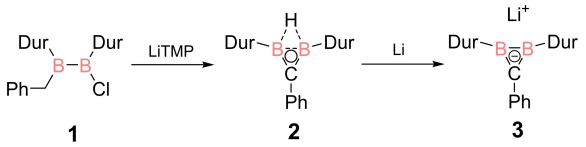

Scheme 3. Synthesis of lithium diboriranide **3** from 1-benzyl-2-chlorodiborane(4) **1** via non-classical diborirane **2** (Dur = duryl = 2,3,5,6-tetramethylphenyl; TMP = 2,2,6,6-tetramethylpiperidide).

boron atoms (δ^{11}B = 24 to 29 ppm).[17] The ^{1}H NMR signal at δ = 7.3 ppm is attributed to the BHB bridge (BHB of preceding 1,2-diduryldiboriranes δ^1H = 7.36 to 7.83 ppm).[17] The substantial broadening caused by the coupling to the two quadrupolar boron nuclei confirms this assignment.

In adaption of the protocol by Berndt et al.,[16,23] the addition of an excess of lithium powder to a solution of **2** in diethylether leads to the formation of diboriranide **3** (Scheme 3), which was isolated as pale-yellow crystals in 60 % yield by crystallization from Et_2O/thf. The ^{11}B NMR spectrum in thf-d_8 shows one broad signal at δ = 44.2 ppm. The deshielding compared to diborirane **2** is probably due to the more pronounced Hückel aromaticity of the B_2C ring system. Accordingly, the ring carbon atom of **3** at δ^{13}C = 151.9 ppm is also deshielded compared to that of diborirane **2** (^{13}C = 135.7 ppm) and thus in range of cyclopropenium cations **I**,[12a] borirenes **II**[10] and other diboriranides.[13] The lithium counter cation in **3** is probably solvent-separated in thf-d_8 as concluded from the absence of significant broadening of the ^{7}Li NMR signal at the unremarkable chemical shift of δ = 0.4 ppm.

Syntheses of diboriranide metal complexes

In view of the 2e3c σ-BHB-bridges that allow for the retention of the $2e^-$ Hückel aromaticity of the three-membered ring of non-classical diboriranes, we envisaged the possibility of similar coordination modes for the metal complexes of diboriranides.

Under the conditions indicated in Table 1, the addition of the appropriate metal halides to lithium diboriranide **3** leads to near quantitative conversion (according to NMR-spectroscopy) to new metal-bridged diboriranides **4** to **7** (Scheme 4).

The reaction of one equivalent of Me_3SnCl with diboriranide **3** in hexane at room temperature affords the tin-bridged diborirane **8**, albeit with small traces (10 %) of

Table 1: Reaction conditions of the addition of reactants to diboriranide **3**. All reactions were carried out at room temperature.

Compound	reactant	Eq.	solvent	duration	yield
4	$AuCl(PPh_3)$	1	thf	15 min	47 %
5	CuCl or $CuI(PPh_3)_3$	0.5	thf	1 h	39 %
6	CuCl	1	thf	12 h	42 %
7	$ZnCl_2$	1	thf	15 min	96 %
8	Me_3SnCl	1	hexane	1 h	50 %

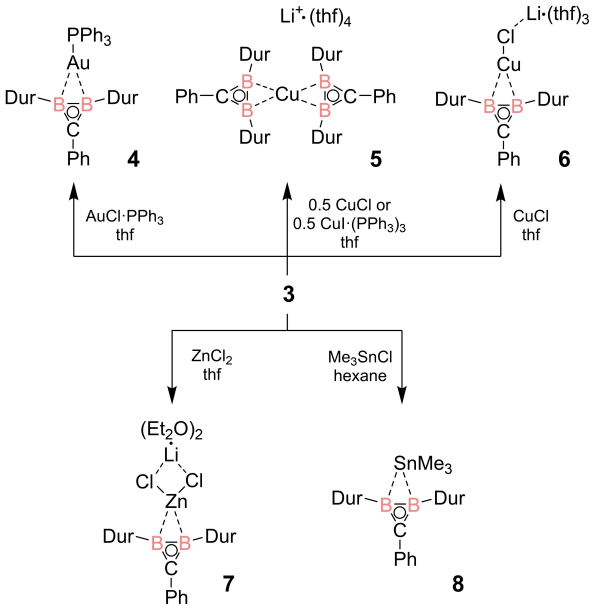

Scheme 4. Syntheses of metal complexes starting from diboriranide **3** (Dur = 2,3,5,6-tetramethylphenyl).

diborirane **2** as a side-product. In all cases, the ^{1}H NMR spectra in solution show only one singlet each for the *ortho*- and *meta*- methyl groups of the duryl substituents confirming their chemical equivalence and therefore symmetric structure of the products in solution on the NMR time scale. The ^{31}P NMR spectrum of the crude product of the addition of 0.5 equivalents of CuI[$(PPh_3)_3$] shows a single signal at $\delta = -4.9$ ppm, which was assigned to free PPh_3,[24] thus suggesting the dissociation of the phosphane-ligand and the formation of cuprate **5**. Indeed, the reaction of CuCl with two equivalents of **3** yields an identical product. In contrast, the ^{31}P NMR spectrum of gold complex **4** shows a downfield-shifted signal at $\delta = 52.2$ ppm, which confirms the retention of PPh_3 in the product. Similar ^{11}B NMR signals are observed in all five complexes (**4**: 37.9 ppm, **5**: 34.7 ppm, **6**: 34.4 ppm, **7**: 32.9 ppm, **8**: 34.0 ppm), somewhat upfield-shifted compared to the precursor, lithium diboriranide **3**.

The ^{119}Sn NMR spectrum of **8** shows a sharp singlet ($\nu_{1/2} = 13.2$ Hz) at $\delta = -38.0$ ppm, in stark contrast to the broad signals of reported stannyl-bridged borane clusters.[25] The absence of coupling of ^{119}Sn to the quadrupolar ^{11}B nuclei suggests a predominant p-character of the 3c2e BSnB bond. The ^{13}C NMR chemical shifts of the ring carbon atoms are all closer to that of diboriranide **3** than to that of diborirane **2** (**4**: 147.8 ppm, **5**: 153.9 ppm, **6**: 151.1 ppm, **7**: 144.0 ppm, **8**: 144.5 ppm, determined at −40 °C to −70 °C, see SI), which indicates a similarly ionic character of the interaction between the B_2C ring and the metal center.

X-Ray diffraction studies

Single crystals of the non-classical diborirane **2** and all diboriranide complexes **3** to **8** were obtained by crystallization from the appropriate solvents (see Supporting Information for conditions).[26] The x-ray diffraction studies confirm the presence of B_2C ring systems in which the B–B bonds are bridged by the hydrogen atom or the incorporated metal fragments, respectively (Figure 1). The cuprate **5** features two η^2-bonded diboriranides, both coordinating edge-on to the spirocyclic copper center with the B–B bonds. The angle between the two B_2C planes indicates almost perpendicularity (B1,B2,C1 and B3,B4,C28: 84.1(2)°). The solvent-separated lithium counter cation of **5** is coordinated by four thf molecules. The B_2C rings, the phenyl-*ipso*-carbon atoms and the B–B-bridging atoms approximately reside in one plane in all complexes **3** to **8**; the largest deviation with 0.23 Å occurs for Li1 of diboriranide **3** (Table 2). The coordination environments of the boron atoms thus approach tetragonal planarity and constitute further examples of violations of the van't Hoff/Le Bel-rule.[27,28] The B–B bond length of 1.769(2) Å in

Table 2: Crystallographic data of diborirane **2** and diboriranide s-, p- and d-block metal complexes **3** to **8**.[a] Duryl-*ipso*-carbon.[b] Angle between B_2C-ringplane and the phenyl-ring plane.[c] Composed of B1,B2,C1, the phenyl-*ipso*-carbon atom and the corresponding metal or hydrogen atom (X).[d] One selected molecule of two in the unit cell.

Compound	B–B [Å]	B–X [Å]	B-Cring [Å]	B-CDur [Å]	B–B-CDur [°][a]	B-Cring-B [°]	dihedral angle [°][b]	Out of plane deviation [Å][c]
2 (X=H)	1.769(2)	1.278(2)	1.442(2)	1.564(2)	155.4(1)	75.6(1)	1.2(1)	0.01 (H1)
		1.309(2)	1.442(2)	1.560(2)	157.2(1)			
3 (X=Li)	1.630(4)	2.402(6)	1.454(4)	1.570(3)	159.3(2)	68.2(2)	16.3(2)	0.23 (Li1)
		2.389(6)	1.455(4)	1.571(3)	159.4(2)			
4 (X=Au)	1.809(4)	2.142(2)	1.442(3)	1.577(3)	167.6(2)	77.8(2)	12.9(1)	0.06 (C1)
		2.242(2)	1.440(3)	1.588(3)	166.8(2)			
5 (X=Cu)	1.690(4)	2.150(3)	1.445(4)	1.577(4)	168.2(2)	71.5(1)	35.2(3)	0.16 (B2)
		2.140(3)	1.448(4)	1.567(4)	167.7(2)			
	1.702(4)	2.147(3)	1.448(4)	1.567(4)	169.5(2)	71.9(2)	1.5(2)	0.20 (B4)
		2.148(3)	1.449(4)	1.573(4)	165.2(2)			
6 (X=Cu)	1.728(5)	2.093(4)	1.450(5)	1.584(4)	165.0(3)	73.3(2)	13.2(2)	0.02 (C1)
		2.071(4)	1.444(5)	1.578(4)	166.1(3)			
7 (X=Zn)[d]	1.719(3)	2.186(2)	1.443(2)	1.577(2)	161.4(1)	73.2(1)	8.2(2)	0.10 (B1)
		2.199(2)	1.440(2)	1.581(2)	163.0(1)			
8 (X=Sn)	1.799(2)	2.462(2)	1.453(2)	1.568(2)	160.1(1)	77.5(1)	10.6(1)	0.08 (B1)
		2.636(2)	1.419(2)	1.559(2)	174.6(1)			

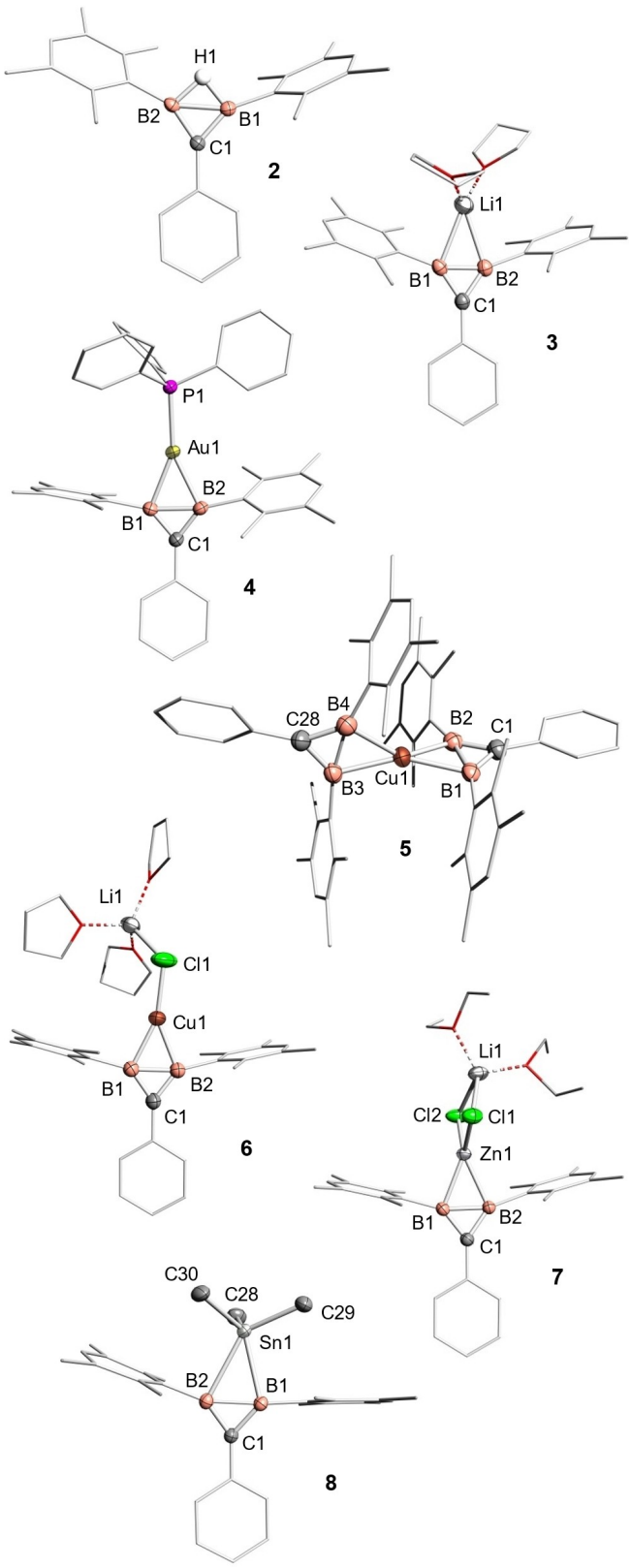

Figure 1. Molecular structures of diborirane **2** and diboriranide metal complexes **3** to **8** in the solid state: gold diboriranide **4**, bis(diboriranide) cuprate **5**, copper diboriranide **6**, zinc diboriranide complex **7**, trimethylstannyl-bridged diboriranide **8**. Most hydrogen atoms, solvent separated counter cation of **5**, and disordered solvent molecules omitted for clarity. Thermal ellipsoids at 50%.[26]

non-classical diborirane **2** is in the typical range of B–B bonds with one bridging hydrogen[17,29] and as such much longer than the one observed in lithium diboriranide **3** (1.630(4) Å).

The latter distance is only slightly longer than neutral B=B double bonds,[30] which is in line with cyclic delocalization of the π electrons, but shorter than most dianionic examples[31] reflecting the absence of Coulomb repulsion. The small dihedral angle (16.3(2)°) between the phenyl group and the diborirane plane in diboriranide **3** agrees with extended π-conjugation although this value is larger than the one in the non-classical diborirane **2** (1.2(1)°).

While the duryl groups at the boron atoms of diborirane **2** are only slightly distorted from the ideal arrangement in an isosceles triangle (Table 2; B1–B2–C_{Dur} 155.4(1)° and B2–B1–C_{Dur} 157.2(1)°), the distortion in diboriranide complexes **3** to **7** becomes progressively more pronounced (159.4(1)° to 169.5(2)°), even approaching linearity in the homoleptic cuprate **5**, which could be attributed to the increased electron density at the copper center.

The diboriranide gold complex **4** shows a nearly linear arrangement of the PPh_3 ligand and the η^2-bonded B–B unit (P1–Au1-centroid B1,B2 176.0(4)°). The B–B σ-bond (B1–B2 1.809(4) Å) is much longer than in lithium diboriranide **3** (B1–B2 1.630(4) Å), but noticeably shorter than in a related azadiboriridine gold complex (1.889 Å).[32] At the same time, the Au–B distances in **4** (B1–Au1 2.214(2) Å, B2–Au1 2.242(2) Å) are elongated compared to the said azadiboridine Au(I) complex (2.118 Å), quite possibly an effect of the electron-withdrawing chloro-ligand at the Au center of the latter. Indeed, the Au–B distances in **4** are comparable to those in boryl (2.21–2.30 Å)[33] and diborene complexes (2.21–2.22 Å),[34] both equally free of electronegative ligands at their Au centers. It should be noted that the azadiboriridine ligand is only of limited value for comparison anyway because of the less effective delocalization of the two π-electrons in the B_2N heterocycle due to the higher electronegativity of the nitrogen center.

Compared to gold complex **4**, the coordination to copper lengthens the B–B distances to a lesser extent: for the homoleptic cuprate **5** (B1–B2 1.690(4), B3–B4 1.702(4) Å) they are in the range of heteroleptic copper complexes of dianionic diboranes(4) (1.68–1.73 Å),[35] the only other example of a cuprate with at least one B–B ligand. The B–Cu distances in **5** (B1–Cu1 2.150(3) Å and B2–Cu1 2.140(3) Å, B3–Cu1 2.147(3) Å, B4–Cu1 2.148(3) Å) are similar to those of neutral (2.10–2.15 Å)[36] and dianionic (2.14–2.23 Å)[35] B=B double bond π-complexes.

The solid-state structure of the heteroleptic monocuprate **6**, which can alternatively be obtained by diboriranide transfer from **5** to a second equivalent of CuCl, revealed the completion of the coordination sphere at the copper center by the chloride ion of one equivalent of LiCl. The lithium cation is in turn coordinated by three thf molecules and the chloride. In line with the presence of the electronegative and thus weakly donating chloride ligand, the B–B bond in **6** is noticeably longer (B1–B2 1.728(5) Å) and the B–Cu bonds (B1–Cu1 2.093(4), B2–Cu1 2.071(4) Å) shorter than in **5**. This observation is confirmed by the molecular structure of the zinc complex **7** in the solid state, which just like **6** contains

one equivalent of LiCl to complete the coordination sphere of the metal center. The B–B bond of **7** (B1–B2 1.719(3) Å) is almost identical to that in **6**. The boron-zinc distances (B1–Zn1 2.186(2) Å, B2–Zn1 2.199(2) Å) in the zinc complex **7** are significantly shorter than in π-complexes of neutral diborenes with zinc dihalides (2.29–2.36 Å),[37] a manifestation of increased Coulomb attraction. The B–B bond lengthening seems to be a direct measure for the σ-donation to the d-block metal in complexes **4** to **7**. Although steric effects cannot be ruled out completely, the σ-donation by the diboriranide to Zn and Cu is approximately the same, but considerably smaller than to Au.

Surprisingly, the x-ray diffraction study on single crystals of tin-bridged diboriranide **8**, also reveals an edge-on coordination of the tin atom to the B–B moiety thus resulting in an expanded five-fold coordination at the Sn1 center as in reported Ph_3Sn-bridged pentaborane(9) clusters.[25a] The B–B bond (B1–B2 1.799(2) Å) is even slightly shorter than in the gold complex **4**. In contrast to the d-block diboriranide complexes, however, the tin atom is noticeably inclined towards one of the boron atoms: the B–Sn bond lengths strongly differ (B1–Sn1: 2.462(2); B2–Sn1 2.636(2) Å), all the while being both longer than the typical B–Sn single bonds of electron precise stannyl boranes (2.28–2.32 Å).[38] While the smaller B1–B2–C_{Dur} angle of 160.1(1)° is in range of the other diboriranide metal complexes **4** to **7**, the larger B2–B1–C_{Dur} angle is with 174.6(1)° remarkably close to linearity.

The structural parameters support a significant contribution by the methyleneborane resonance structure **8′** (Scheme 5). While there is no indication for such a lowering of the symmetry in solution, this may well be due to a fast exchange on the ^{1}H NMR time scale even at −40 °C.

DFT calculations

The electronic structure of the diborirane **2** and the diboriranide metal complexes **3**, **4**, **5**, **7** and **8** was investigated by DFT calculations at the B3LYP/def2tzvpp level of theory. The Kohn–Sham molecular orbitals (MOs) were calculated from structures that were optimized at the BP86/def2SVP level of theory. Whereas the optimized structures of **2**, **3**, **4**, **5**, **7** and **8** match the crystal structures reasonably well, the experimentally determined Cl–Cu–BB(centroid) angle in the mono(diboriranide)cuprate **6** was not reproduced by the computations, presumably due to packing effects in the solid state (see SI). Therefore, the MOs of **6** are derived from a single point calculation using the coordinates experimentally obtained from the solid state structure.

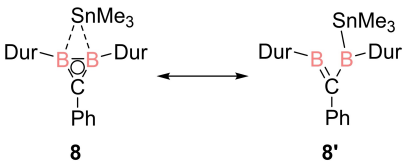

Scheme 5. Tin bridged diboriranide complex **8** and methyleneborane resonance structure **8′**.

Whereas the all-bonding combination of the π-orbitals of the B_2C ring represents the HOMO in case of the diborirane **2**, the σ-donation to the Li^+ counterion is raised to above the corresponding π-orbital in **3** (Figure 2 and SI). Natural bond orbital (NBO) analyses yields a 3c2e interaction of nearly perfect π-symmetry for both **2** and **3** (at least 99.7 % p-character for all involved atoms). In addition, the non-classical diborirane **2** features the expected BHB 3c2e σ-interaction which is approximately composed of sp^3-hybrids at the boron centers (see SI). The disappearance of the BHB 3c2e σ-bond in diboriranide **3** in favor of a classical 2e2c σ-bond is further confirmed by increasing Wiberg bond indexes of the B–B bond from diborirane **2** (0.53) to diboriranide **3** (1.06). Concomitantly, the positive charges at the boron atoms decrease according to natural population analysis (NPA; **2**: B1: +0.49, B2: +0.48; **3**: B1: +0.20, B2: +0.19), illustrating the higher electron density in the B_2C ring system in diboriranide **3** compared to diborirane **2**. As expected, the main negative charge is located at the carbon atom of the ring system (**2**: −0.62, **3**: −0.60).

The HOMO of the gold(I) complex **4** (Figure 3) is an antibonding combination of the σ-orbital of the B–B moiety and the d_{z^2} orbital of the metal center. The HOMO−1 corresponds to the all-bonding aromatic π-system delocalized across the B_2C ring with only very minor contributions by the Au center, which further supports the essentially σ-only coordination. The LUMO of **4** is mainly composed of an antibonding phosphorus-centered orbital of the PPh_3 ligand with stabilizing interactions to the π-system of one of the three phenyl groups at phosphorus.

In contrast to gold complex **4**, both the homoleptic and heteroleptic cuprates **5** and **6**, respectively, exhibit a LUMO resulting from the constructive interaction of the π*-system at the B_2C ring with the pending phenyl ring. The HOMO of both cuprate complexes **5** and **6** is similar to that of the gold complex **4** consisting of an antibonding combination of the σ-orbital of the B–B moiety and the d_{z^2} orbital of the metal center. Here as well, the HOMO−1 represents the all-bonding delocalized π-system of the B_2C ring with minor

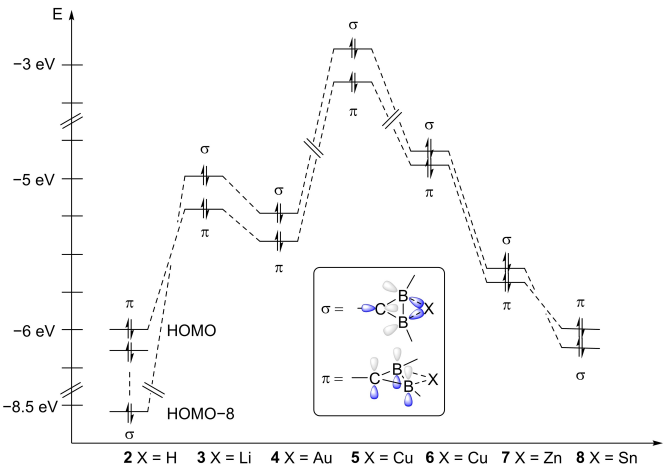

Figure 2. Relative energies of the HOMOs and HOMOs−1 of diborirane **2** and diboriranide derivatives **3** to **8**.

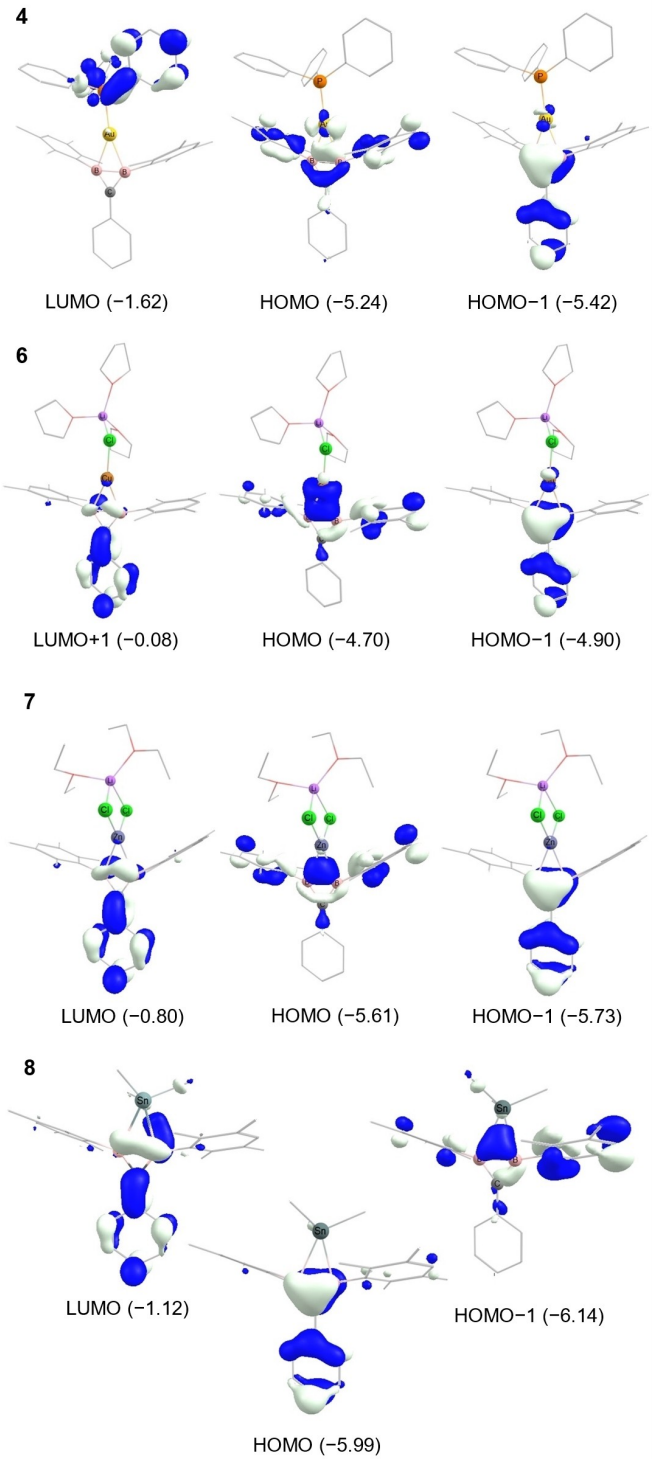

Figure 3. Selected frontier orbitals of diboriranide metal complexes **4** and **6** to **8** (energy in eV, contour value = 0.05).

contributions by the copper centers. While the LUMO of cuprate **6** is composed of σ*-orbitals at the solvent molecules (see SI), the LUMO + 1 of **6** corresponds to the LUMO of bis(diboriranide) **5** being mainly composed of the π*-system at the boron atoms and the phenyl ring.

The HOMO of zincate **7** represents the donation of σ-electrons from the boron atoms to the zinc atom. In contrast to the corresponding orbitals of the complexes discussed above, it does not show contributions of any zinc-centred orbital although the HOMO−1 once more represents the diboriranide π-system.

Most notably, the energetic order of occupied frontier orbitals is reversed in the Me_3Sn-bridged **8**: the HOMO represents the π-system and the HOMO−1 the σ-donation to the tin center (Figure 2). The LUMO of **8** represents the π*-system at the boron atoms and is of comparably low energy (−1.12 eV). The increased energy of the π-orbitals of **8** lends further support to the disturbance of cyclic delocalization by a significant contribution of resonance structure **8′** (Scheme 5).

For further confirmation of the aromaticity of diborirane **2** and diboriranide complexes **3** to **8**, nucleus independent chemical shifts (NICS) were calculated in the geometrical center of the B_2C moieties at the B3LYP/def2TZVP level of theory (Table 3). The obtained values for NICS(0) are similar to that of the cyclopropenium cation, which we calculated at the same level of theory for comparison (NICS(0) = −23.2).[39] In order to minimize the effect of localized ring currents as well as the shielding by the σ-framework, NICS were also calculated 1 Å above and below the B_2C ring plane.[40] All values for NICS(1/−1) in the range of −10.6 to −13.3 are only slightly lower than that of the cyclopropenium cation (NICS(1) = −14.9)[39] and thus confirm the 2π-aromaticity of the three membered ring systems in **2** to **8** and its essential independency from the nature of the coordinated metal. Notably, even the coordination of the Me_3Sn group in **8** does not seem to exert an adverse effect on the magnetically induced ring current.

Conclusion

We have disclosed a straightforward synthetic strategy to access diboriranes in two steps from a readily available 1,2-dichlorodiborane(4). Unlike in previously reported diboriranes, a phenyl group is attached to the ring carbon atom; its coplanarity allows for π-conjugation with the B_2C ring plane for the first time, thus offering new perspectives regarding the incorporation of non-classical diborirane motifs into extended π-systems. The nearly planar anti-van't Hoff/Le Bel-geometry at the boron centers is retained upon reduction to lithium diboriranide **3** and - more importantly - also upon complexation to various d-block elements, namely gold (**4**), copper (**5**, **6**), and zinc (**7**). The diboriranide binds to the p- and d-block metal complexes in this very same plane, essentially by σ-only coordination thus leaving the π-system mostly unperturbed. In case of the stannyl-bridged diboriranide **8**, however, crystallographic evidence suggests a weakening of the cyclic delocalization as one of the two Sn–B distances is substantially elongated to localize the bonding to some extent and hence lower the degree of hypercoordination at the tin-center, which is considered to be unfavorable in the absence of electronegative substituents.

Table 3: Different values for NICS (in ppm) of diborirane **2** and diboriranide derivatives **3** to **8**. Calculated from the geometric center of the B_2C plane (NICS(0)) and 1 Å above and below the B_2C ring plane (NICS(1/−1)).

Compound	NICS(0)	NICS(1/−1)
2	−25.3	−12.6/−12.8
3	−19.5	−12.1/−12.7
4	−19.9	−10.6/−11.7
5	−19.9	−12.4/−12.7
	−20.1	−12.9/−13.2
6	−20.4	−11.9/−12.5
7	−23.3	−12.2/−12.7
8	−22.8	−13.3/−10.7

The scope of the new method, in particular with regards to the tolerance of functional groups as well as to the further extension of the π-conjugated system is currently under investigation in our laboratory.

Acknowledgements

We gratefully acknowledge the funding by Saarland University. We thank Dr. Diego Andrada for assistance with computations, helpful discussions, and access to his computational cluster. We acknowledge the Service Center X-ray Diffraction established with financial support from Saarland University and the Deutsche Forschungsgemeinschaft (INST 256/506-1). Open Access funding enabled and organized by Projekt DEAL.

Conflict of Interest

The authors declare no conflict of interest.

Data Availability Statement

The data that support the findings of this study are available in the supplementary material of this article.

Keywords: Aromatics · Boron · Coordination Chemistry · Transition Metals

[1] a) H. Wadepohl, *Angew. Chem. Int. Ed. Engl.* **1992**, *31*, 247–262; b) D. Braga, P. J. Dyson, F. Grepioni, B. F. G. Johnson, *Chem. Rev.* **1994**, *94*, 1585–1620; c) K. M. Wedderburn, S. Bililign, M. Levy, R. Gdanitz, *Chem. Phys.* **2006**, *326*, 600–604.

[2] L. D. Field, C. M. Lindall, A. F. Masters, G. K. B. Clentsmith, *Coord. Chem. Rev.* **2011**, *255*, 1733–1790.

[3] P. L. Pauson, G. H. Smith, J. H. Valentine, *J. Chem. Soc. C* **1967**, 1061–1065.

[4] a) C.-W. So, D. Watanabe, A. Wakamiya, S. Yamaguchi, *Organometallics* **2008**, *27*, 3496–3501; b) G. E. Herberich, B. Buller, B. Heßner, W. Oschmann, *J. Organomet. Chem.* **1980**, *195*, 253–259; c) J. He, F. Rauch, M. Finze, T. B. Marder, *Chem. Sci.* **2021**, *12*, 128–147.

[5] For selected examples of bora and boratabenzenes see: a) G. E. Herberich, G. Greiss, H. F. Heil, *Angew. Chem. Int. Ed. Engl.* **1970**, *9*, 805–806; b) G. E. Herberich, H. Ohst, *Adv. Organomet. Chem.* **1986**, *25*, 199–236; c) A. J. Ashe III, P. Shu, *J. Am. Chem. Soc.* **1971**, *93*, 1804–1805; d) R. Boese, N. Finke, J. Henkelmann, G. Maier, P. Paetzold, H. P. Reisenauer, G. Schmid, *Chem. Ber.* **1985**, *118*, 1644–1654; e) G. C. Fu, *Adv. Organomet. Chem.* **2001**, *47*, 101–119.

[6] For selected examples of dibora- and diboratabenzenes see: a) G. E. Herberich, B. Heßner, M. Hostalek, *Angew. Chem. Int. Ed. Engl.* **1986**, *25*, 642–643; b) G. E. Herberich, B. Heßner, M. Hostalek, *J. Organomet. Chem.* **1988**, *355*, 473–484; c) W. Weinmann, H. Pritzkow, W. Siebert, *Chem. Ber.* **1994**, *127*, 611–613; d) C. Balzereit, H.-J. Winkler, W. Massa, A. Berndt, *Angew. Chem. Int. Ed. Engl.* **1994**, *33*, 2306–2308; e) G. E. Herberich, B. Heßner, *Chem. Ber.* **1982**, *115*, 3115–3127; f) J. W. Taylor, A. McSkimming, C. F. Guzman, W. H. Harman, *J. Am. Chem. Soc.* **2017**, *139*, 11032–11035; g) M. Arrowsmith, J. Böhnke, H. Braunschweig, M. A. Celik, C. Claes, W. C. Ewing, I. Krummenacher, K. Lubitz, C. Schneider, *Angew. Chem. Int. Ed.* **2016**, *55*, 11271–11275; h) Q. Sun, C. G. Daniliuc, C. Mück-Lichtenfeld, G. Kehr, G. Erker, *Angew. Chem. Int. Ed.* **2022**, *61*, e202205565.

[7] For selected examples of borepins see: a) A. J. Ashe III, F. J. Drone, C. M. Kausch, J. Kroker, S. M. Al-Taweel, *Pure Appl. Chem.* **1990**, *62*, 513–517; b) A. J. Ashe, III, W. Klein, R. Rousseau, *Organometallics* **1993**, *12*, 3225–3231; For selected examples of boron containing heterocycles see: c) C. W. Allen, D. E. Palmer, *J. Chem. Educ.* **1978**, *55*, 497–500; d) G. E. Herberich, *Comprehensive Organometallic Chemistry II*, *Vol. 1*, Elsevier, Amsterdam, **1995**, chap. 5, pp. 197–216; e) B. Su, R. Kinjo, *Synthesis* **2017**, *49*, 2985–3034; f) J. T. Goettel, H. Braunschweig, *Coord. Chem. Rev.* **2019**, *380*, 184–200; g) U. M. Dzhemilev, L. I. Khusainova, K. S. Ryazanov, L. O. Khafizova, *Russ. Chem. Bull. Int. Ed.* **2021**, *70*, 1851–1892.

[8] a) K.-F. Wörner, W. Siebert, *Z. Naturforsch. B* **1989**, *44*, 1211–1213; b) D. A. Loginov, D. V. Muratov, P. V. Petrovskii, Z. A. Starikova, M. Corsini, F. Laschi, F. D. B. Fabrizi, P. Zanello, A. R. Kudinov, *Eur. J. Inorg. Chem.* **2005**, 1737–1746; c) W. Siebert, A. R. Kudinov, P. Zanello, M. Y. Antipin, V. V. Scherban, A. S. Romanov, D. V. Muratov, Z. A. Starikova, M. Corsini, *Organometallics* **2009**, *28*, 2707–2715; d) D. A. Loginov, D. V. Muratov, Y. V. Nelyubina, J. Laskova, A. R. Kudinov, *J. Mol. Catal. A* **2017**, *426*, 393–397.

[9] a) P. D. Frisch, G. P. Khare, *J. Organomet. Chem.* **1977**, *142*, 61–64; b) A. Keasey, P. M. Maitlis, *J. Chem. Soc. Dalton Trans.* **1978**, 1830–1839; c) C. Mealli, S. Midollini, S. Moneti, L. Sacconi, *J. Organomet. Chem.* **1981**, *205*, 273–279; d) R. P. Hughes, D. S. Tucker, A. L. Rheingold, *Organometallics* **1994**, *13*, 4664–4666; e) M. S. Morton, J. P. Selegue, *J. Organomet. Chem.* **1999**, *578*, 133–143; f) K. Komatsu, T. Kitagawa, *Chem. Rev.* **2003**, *103*, 1371–1428; g) C. Jandl, K. Öfele, A. Pöthig, *Organometallics* **2017**, *36*, 4348–4350; h) D. N. Platonov, D. N. Kholodkov, I. K. Goncharova, M. A. Belaya, Y. V. Tkachev, P. V. Dorovatovskii, A. D. Volodin, A. A. Korlyukov, Y. V.

Tomilov, A. V. Arzumanyan, R. A. Novikov, *Organometallics* **2021**, *40*, 3876–3885.

[10] a) H. Braunschweig, T. Herbst, D. Rais, F. Seeler, *Angew. Chem. Int. Ed.* **2005**, *44*, 7461–7463; b) H. Braunschweig, T. Herbst, D. Rais, S. Ghosh, T. Kupfer, K. Radacki, A. G. Crawford, R. M. Ward, T. B. Marder, I. Fernández, G. Frenking, *J. Am. Chem. Soc.* **2009**, *131*, 8989–8999.

[11] a) H. Braunschweig, Q. Ye, K. Radacki, *Chem. Commun.* **2009**, 6979–6981; b) H. Braunschweig, Q. Ye, K. Radacki, P. Brenner, G. Frenking, S. De, *Inorg. Chem.* **2011**, *50*, 62–71; c) H. Braunschweig, Q. Ye, K. Radacki, T. Kupfer, *Dalton Trans.* **2011**, *40*, 3666–3670; d) H. Braunschweig, A. Damme, R. D. Dewhurst, S. Ghosh, T. Kramer, B. Pfaffinger, K. Radacki, A. Vargas, *J. Am. Chem. Soc.* **2013**, *135*, 1903–1911.

[12] a) X. Meng, T. P. Fehlner, A. L. Rheingold, *Organometallics* **1990**, *9*, 534–536; b) H. Braunschweig, R. D. Dewhurst, *Dalton Trans.* **2011**, *40*, 549–558; c) H. Braunschweig, R. D. Dewhurst, K. Radacki, C. W. Tate, A. Vargas, *Angew. Chem. Int. Ed.* **2014**, *53*, 6263–6266.

[13] a) R. Wehrmann, H. Meyer, A. Berndt, *Angew. Chem. Int. Ed. Engl.* **1985**, *24*, 788–790; b) H. Meyer, G. Schmidt-Lukasch, G. Baum, W. Massa, A. Berndt, *Z. Naturforsch. B* **1988**, *43*, 801–806.

[14] a) D. Scheschkewitz, A. Ghaffari, P. Amseis, M. Unverzagt, G. Subramanian, M. Hofmann, P. V. R. Schleyer, H. F. Schaefer, III, G. Geiseler, W. Massa, A. Berndt, *Angew. Chem. Int. Ed.* **2000**, *39*, 1272–1275; b) W. Lößlein, H. Pritzkow, P. V. R. Schleyer, L. R. Schmitz, W. Siebert, *Eur. J. Inorg. Chem.* **2001**, 1949–1956; c) N. Li, B. Wu, C. Yu, T. Li, W.-X. Zhang, Z. Xi, *Angew. Chem. Int. Ed.* **2020**, *59*, 8868–8872.

[15] T. Kupfer, H. Braunschweig, K. Radacki, *Angew. Chem. Int. Ed.* **2015**, *54*, 15084–15088.

[16] M. Unverzagt, PhD thesis, University of Marburg, **1997**.

[17] a) D. Steiner, C. Balzereit, H.-J. Winkler, N. Stamatis, W. Massa, A. Berndt, M. Hoffmann, P. V. R. Schleyer, *Angew. Chem. Int. Ed. Engl.* **1994**, *33*, 2303–2306; b) M. Menzel, D. Steiner, H.-J. Winkler, D. Schweikart, S. Mehle, S. Fau, G. Frenking, W. Massa, A. Berndt, *Angew. Chem. Int. Ed. Engl.* **1995**, *34*, 327–329; c) C. Präsang, Y. Sahin, M. Hofmann, G. Geiseler, W. Massa, A. Berndt, *Eur. J. Inorg. Chem.* **2008**, 5046–5055.

[18] A. Hübner, T. Kaese, M. Diefenbach, B. Endeward, M. Bolte, H.-W. Lerner, M. C. Holthausen, M. Wagner, *J. Am. Chem. Soc.* **2015**, *137*, 3705–3714.

[19] Y. Wang, X. Zhang, J. Han, Q. Li, R. Wei, D. A. Ruiz, L. L. Liu, C.-H. Tung, L. Kong, *Angew. Chem. Int. Ed.* **2022**, *61*, e202117053.

[20] A. Berndt, *Angew. Chem. Int. Ed. Engl.* **1993**, *32*, 985–1009.

[21] H. Hommer, H. Nöth, J. Knizek, W. Ponikwar, H. Schwenk-Kircher, *Eur. J. Inorg. Chem.* **1998**, 1519–1527.

[22] K. V. Baker, J. M. Brown, N. Hughes, A. J. Skarnulis, A. Sexton, *J. Org. Chem.* **1991**, *56*, 698–703.

[23] D. Steiner, H. J. Winkler, C. Balzereit, T. Happel, W. Massa, A. Berndt, M. Hofmann, G. Subramanian, P. V. R. Schleyer, *Angew. Chem. Int. Ed. Engl.* **1996**, *35*, 1990–1992.

[24] A. C. Vetter, K. Nikitin, D. G. Gilheany, *Chem. Commun.* **2018**, *54*, 5843–5846.

[25] a) D. K. Srivastava, N. P. Rath, L. Barton, *Organometallics* **1992**, *11*, 2263–2273; b) H. Fang, D. Zhao, L. Brammer, L. Barton, *J. Chem. Soc. Chem. Commun.* **1994**, 1531–1532; c) H. Fang, D. Zhao, N. P. Rath, L. Brammer, L. Barton, *Organometallics* **1995**, *14*, 1700–1711.

[26] Deposition numbers 2269482 (for **1**), 2269486 (for **2**), 2269489 (for **3**), 2269491 (for **4**), 2269493 (for **5**), 2269495 (for **6**), 2269501 (for **7**), 2269505 (for **8**). contain the supplementary crystallographic data for this paper. These data are provided free of charge by the joint Cambridge Crystallographic Data Centre and Fachinformationszentrum Karlsruhe Access Structures service.

[27] a) R. Hoffmann, R. W. Alder, C. F. Wilcox Jr., *J. Am. Chem. Soc.* **1970**, *92*, 4992–4993; b) R. Hoffmann, *Pure Appl. Chem.* **1971**, *28*, 181–194.

[28] For selected examples of anti-van't Hoff/Le Bel-geometry see: a) M. Driess, J. Aust, K. Merz, C. van Wüllen, *Angew. Chem. Int. Ed.* **1999**, *38*, 3677–3680; b) R. Keese, *Chem. Rev.* **2006**, *106*, 4787–4808; c) M. J. Cowley, V. Huch, D. Scheschkewitz, *Chem. Eur. J.* **2014**, *20*, 9221–9224; d) F. Ebner, L. Greb, *J. Am. Chem. Soc.* **2018**, *140*, 17409–17412; e) F. Ebner, H. Wadepohl, L. Greb, *J. Am. Chem. Soc.* **2019**, *141*, 18009–18012; f) F. Ebner, L. Greb, *Chem* **2021**, *7*, 2151–2159; g) P. Ghana, J. Rump, G. Schnakenburg, M. I. Arz, A. C. Filippou, *J. Am. Chem. Soc.* **2021**, *143*, 420–432; h) C. Shan, S. Dong, S. Yao, J. Zhu, M. Driess, *J. Am. Chem. Soc.* **2023**, *145*, 7084–7089.

[29] X. Mao, J. Zhang, Z. Lu, Z. Xie, *Chem. Sci.* **2022**, *13*, 3009–3013.

[30] For examples of neutral B=B double bonds see a) Y. Wang, B. Quillian, P. Wei, C. S. Wannere, Y. Xie, R. B. King, H. F. Schaefer III, P. V. R. Schleyer, G. H. Robinson, *J. Am. Chem. Soc.* **2007**, *129*, 12412–12413; b) Y. Wang, B. Quillian, P. Wei, Y. Xie, C. S. Wannere, R. B. King, H. F. Schaefer, III, P. V. R. Schleyer, G. H. Robinson, *J. Am. Chem. Soc.* **2008**, *130*, 3298–3299; c) H. Braunschweig, R. D. Dewhurst, K. Hammond, J. Mies, K. Radacki, A. Vargas, *Science* **2012**, *336*, 1420–1422; d) P. Bissinger, H. Braunschweig, A. Damme, T. Kupfer, A. Vargas, *Angew. Chem. Int. Ed.* **2012**, *51*, 9931–9934; e) W. Lu, Y. Li, R. Ganguly, R. Kinjo, *J. Am. Chem. Soc.* **2017**, *139*, 5047–5050.

[31] For examples of anionic B–B π-bonds see: a) H. Klusik, A. Berndt, *Angew. Chem. Int. Ed. Engl.* **1981**, *20*, 870–871; b) W. J. Grigsby, P. P. Power, *Chem. Eur. J.* **1997**, *3*, 368–375; c) A. Moezzi, R. A. Bartlett, P. P. Power, *Angew. Chem. Int. Ed. Engl.* **1992**, *31*, 1082–1083; d) A. Moezzi, M. Olmstead, P. P. Power, *J. Am. Chem. Soc.* **1992**, *114*, 2715–2717; e) P. P. Power, *Inorg. Chim. Acta* **1992**, *198–200*, 443–447; f) W. J. Grigsby, P. P. Power, *Chem. Commun.* **1996**, 2235–2236.

[32] R. Shang, S. Saito, J. O. C. Jimenez-Halla, Y. Yamamoto, *Dalton Trans.* **2018**, *47*, 5181–5188.

[33] H. Braunschweig, A. Damme, R. D. Dewhurst, T. Kramer, S. Östreicher, K. Radacki, A. Vargas, *J. Am. Chem. Soc.* **2013**, *135*, 2313–2320.

[34] W. Lu, R. Kinjo, *Chem. Eur. J.* **2018**, *24*, 15656–15662.

[35] S. Akiyama, S. Ikemoto, S. Muratsugu, M. Tada, M. Yamashita, *Organometallics* **2020**, *39*, 500–504.

[36] M. Dömling, T. E. Stennett, A. Belyaev, B. Hupp, C. Claes, S. Ullrich, S. Endres, E. Freytag, T. Kramer, T. Kupfer, F. Schorr, T. Thiess, M. Arrowsmith, A. Steffen, H. Braunschweig, *Inorg. Chem.* **2022**, *61*, 14058–14066.

[37] S. R. Wang, M. Arrowsmith, H. Braunschweig, R. Dewhurst, M. Dömling, J. D. Mattock, C. Pranckevicius, A. Vargas, *J. Am. Chem. Soc.* **2017**, *139*, 10661–10664.

[38] T. Habereder, H. Nöth, *Z. Anorg. Allg. Chem.* **2001**, *627*, 789–796.

[39] Previously a value of −23.5 ppm had been reported for NICS(0) of $C_3H_3^+$ at a slightly different level of theory: C. Foroutan-Nejad, S. Shabazian, P. Rashidi-Ranjbar, *Phys. Chem. Chem. Phys.* **2010**, *12*, 12630–12637.

[40] P. V. R. Schleyer, H. Jiao, N. J. R. V. E. Hommes, V. G. Malkin, O. L. Malkina, *J. Am. Chem. Soc.* **1997**, *119*, 12669–12670.

Manuscript received: June 20, 2023
Accepted manuscript online: July 31, 2023
Version of record online: August 28, 2023